Supplementary information

Fluorescent sensing and Magnetic properties of three coordination polymers based on 6-(3,5-dicarboxylphenyl)nicotinic acid and pyridine/imidazole linkers

Jie Zhang[a], Lingling Gao[a], Yang Wang[a], Lijun, Zhai[a], Xiaoqing Wang[a], Xiaoyan Niu [a] and Tuoping Hu*[a]

Table S1. Crystallographic data for **1**, **2** and **3**.

Complex	**1**	**2**	**3**
Empirical formula	$C_{24}H_{15}N_3NiO_6$	$C_{112}H_{94}N_{18}Ni_3O_{21}$	$C_{76}H_{80}Cu_3N_{16}O_{20}$
Formula weight	500.10	2204.18	1728.18
Crystal system	Monoclinic	Triclinic	Monoclinic
Space group	*P2/c*	*P*$\bar{1}$	$P2_1/c$
a [Å]	11.2448(14)	10.107 (5)	14.0116(18)
b [Å]	10.0674(13)	13.460 (8)	19.843(3)
c [Å]	24.394(3)	23.318 (14)	15.3662(19)
α [º]	90	92.653 (7)	90
β [º]	93.663(2)	95.757 (9)	109.191(3)
γ [º]	90	109.755 (6)	90
V [Å^3]	2755.9(6)	2960 (3)	1733.23(18)
Z	4	1	2
*D*c / (g·cm^{-3})	1.205	1.237	1.438
F(000)	1024.0	1144.0	1790.0
μ(Mo *K*α) / mm^{-1}	0.742	0.829	0.859
Reflections collected	14763	280982	22948
θ range for data collection / (°)	1.623-25.682	2.5-25.027	1.73-26.377
Independent reflections (R_{int})	5237 (0.1027)	4844 (0.0340)	8163(0.0580)
Data / restraints / parameters	5237/177/363	4844/10/412	8163/54/522
Gof	0.909	1.123	1.028
R_1, wR_2 [$I>2\sigma(I)$]^{ab}	0.0569, 0.1174	0.0417, 0.0864	0.0059,0.1584
R_1, wR_2 (all data)^a	0.1241, 0.1414	0.0452, 0.0874	0.0961,0.1818
Largest diff. Peak and hole[e·Å^{-3}]	0.57 and -0.57	0.59 and -1.11	0.93 and -0.64
CCDC number	1886813	1886814	1886815

$^aR_1=\Sigma||F_o|-|F_c||/\Sigma|F_o|$. $^bwR_2 = \{[\Sigma w(F_o2-F_c^2)^2/\Sigma w(F_o^2)^2]\}^{1/2}$.

Table. S2 Selected bond lengths/Å and bond angles/ºfor complex (**1**), (**2**) and (**3**)

Complex 1					
Ni1–O1^A	2.162(3)	Ni1–O3	2.049(3)	Ni1–N1	2.085(4)
Ni1–O5^B	2.069(3)	Ni1–O2^A	2.084(3)	Ni1–N2^C	2.070(4)
O5^{ii}-Ni1-O1^A	152.19(12)	O3–Ni1–O2^A	156.73(12)	N1–Ni1–O1^A	90.59(14)
O5^{ii}-Ni1-O2^A	89.98(12)	O3–Ni1–N1	91.26(14)	N23–Ni1–O1^A	89.46(13)

O5^{ii}–Ni1–N1	89.44(14)	O3–Ni1–N2^{C}	89.77(13)	N23–Ni1–O2^{A}	88.76(13)
O5^{B}–Ni1–N2^{C}	90.03(14)	O2^{A}–Ni1–O1^{A}	62.21(11)	N23–Ni1–N1	178.97(15)
O3–Ni1–O1^{A}	94.56(11)	O2^{A}–Ni1–N1	90.35(14)	O3–Ni1–O5^{B}	113.24(12)
Symmetry codes: ^{A}1+*x,1+y,+z;* ^{B}+*x,1-y,-1/2+z;* ^{C}*-1+x,+y+z;*+z					
Complex 2					
Ni1–N5^{A}	2.128 (4)	Ni1–O1	2.067 (3)	Ni1–O1^{A}	2.067 (3)
Ni1–O2W	2.089 (4)	Ni1–O2W^{A}	2.090 (4)	NA2–N1^{C}	2.105 (3)
Ni2–O3	2.163 (3)	Ni2–O3W	2.091 (3)	Ni2–O4	2.094 (3)
Ni2–O5^{D}	2.005 (3)				
N5^{A}–Ni1–N5	180.0	O1^{A}–Ni1–N5	90.01 (14)	O1^{A}–Ni1–N5^{A}	89.99 (14)
O1–Ni1–N5	89.99 (14)	O1–Ni1–N5^{A}	90.01 (14)	O1^{A}–Ni1–O1	180.0
O1–Ni1–O2W^{A}	88.40 (14)	O1^{A}–Ni1–O2W^{A}	91.60 (14)	O1–Ni1–O2W	91.60 (14)
O1^{i}–Ni1–O2W	88.40 (14)	O2W^{i}–Ni1–N5	90.10 (15)	O2W^{A}–Ni1–N5^{A}	88.90 (15)
O2W–Ni1–N5^{A}	91.10 (15)	O2W–Ni1–N5	88.90 (15)	O2W^{A}–Ni1–O2W	180.0 (2)
N1^{C}–Ni2–O3	88.05 (13)	N4–Ni2–N1^{C}	178.97 (14)	N4–Ni2–O3	90.92 (12)
N4–Ni2–O3W	91.75 (13)	O3W–Ni2–N1^{C}	89.26 (13)	O3W–Ni2–O3	164.93 (10)
O4–Ni2–N1^{C}	92.65 (12)	O4–Ni2–N4	86.91 (12)	O4–Ni2–O3	62.39 (11)
O4–Ni2–O3W	102.96 (11)	O5^{D}–Ni2–N1^{C}	87.49 (12)	O5^{D}–Ni2–N4	92.62 (12)
O5^{D}–Ni2–O3	98.65 (11)	O5^{D}–Ni2–O3W	96.04 (12)	O5^{D}–Ni2–O4	161.01 (12)
Symmetry codes: ^{A}+X,-1+Y,+Z; ^{B}2-X,2-Y,1-Z; ^{C}+X,1+Y,+Z; ^{D}-1+X,+Y,+Z; ^{E}1+X,+Y,+Z					
Complex 3					
Cu1–O1 ^{A}	1.946(2)	Cu2–O3^{B}	1.956(3)	Cu1–N2 ^{A}	1.965(3)
Cu1–O1	1.946(2)	Cu2–O5	1.924(3)	Cu1–N2	1.965(3)
Cu2–N8 ^{C}	1.987(4)	Cu2–N5	1.986(4)		
O11–Cu1–O1	180.00(9)	O1–Cu1–N2	90.22(12)	O32–Cu2–N5	89.41(13)
O1—Cu1–N2^{A}	89.78(12)	O11–Cu1–N2	89.78(12)	O32–Cu2–N8^{C}	90.36(14)
O11–Cu1–N2^{A}	90.22(12)	N21–Cu1–N2	180	O5–Cu2–O3^{B}	167.82(12)
O5–Cu2–N5	91.49(13)	O5–Cu2–N8^{C}	91.05(13)	N5–Cu2–N8^{C}	168.99(15)

Symmetry codes: ^{A}-x,1-y,-z; ^{B}1-x,-1/2+y,3/2-x;^{C}1+x,+y,+z;^{D}1-x,1/2+y,3/2-z; ^{E}1-x,1-y,-z; ^{F}-1+x,+y,+z.

Table S3. Related parameters in the sensing of nitroaromatics/Fe^{3+}ions in **3**.

	Quenching rate	Exponential equation	K_{sv} (M^{-1})	The detection limit
NT	98.96% (0.200 mM)	I_0/I=1.54e [NT]/0.08-0.38	4.2×10^{3}	0.69×10^{-3}
NA	91.53% (0.200 mM)	I_0/I=2.92e [NA]/0.13-1.83	4.0×10^{3}	0.73×10^{-3}
NB^{+}	85.98% (0.300 mM)	I_0/I=0.77e [NB]/0.24-2.30	1.9×10^{3}	1.5×10^{-3}
NP	86.17% (0.300 mM)	I_0/I=2.78e [NP]/0.17-1.82	2.3×10^{3}	1.2×10^{-4}
Fe^{3+}	96.08% (0.06 mM)	I_0/I=0.11e [Fe3+]/0.01+1.26	5.8×10^{3}	7.2×10^{-4}

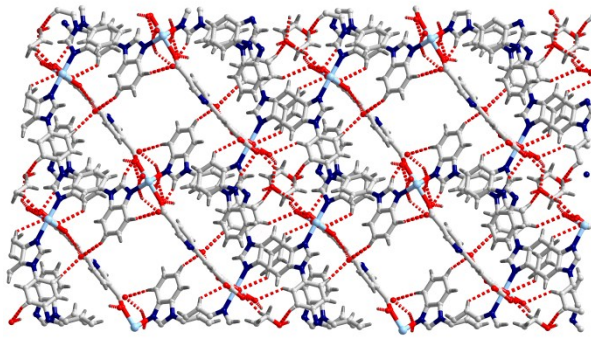

Figure S1. The hydrogen bonds between adjacent 2D sheets.

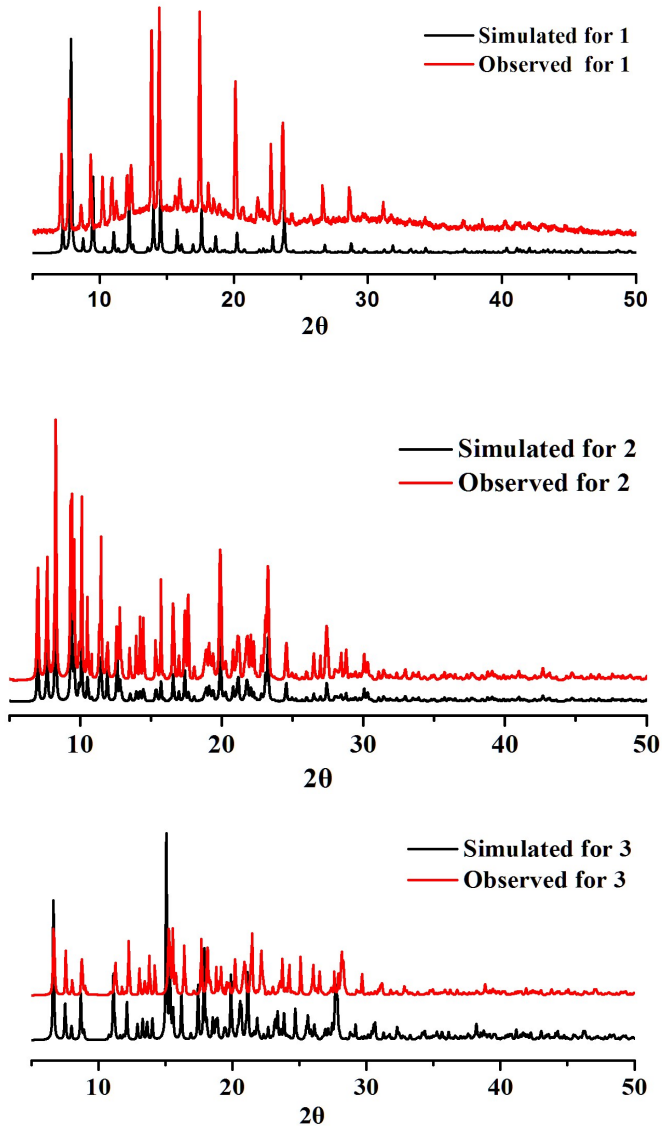

Figure S2. PXRD patterns of the series complexes. Black: Simulated from the X–ray single–crystal data; Red: observed for the as–synthesized solids.

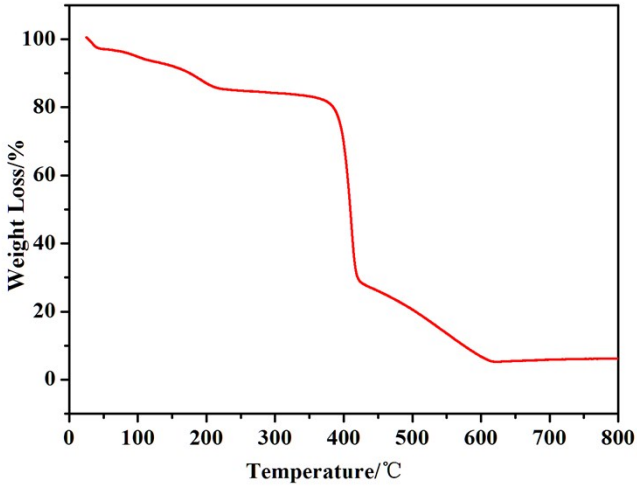

Figure S3. The TG curve of complex **1**.

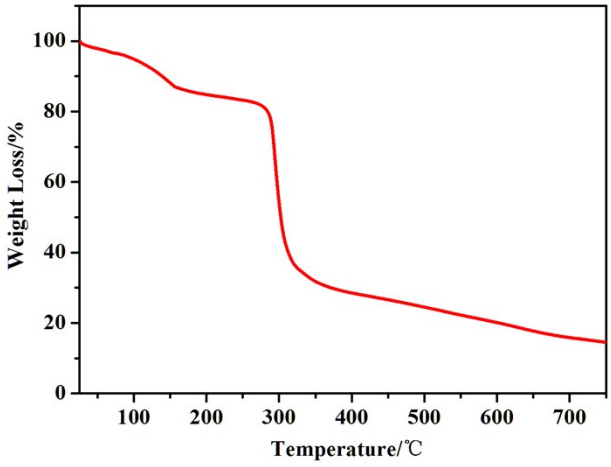

Figure S4. The TG curve of complex **2**.

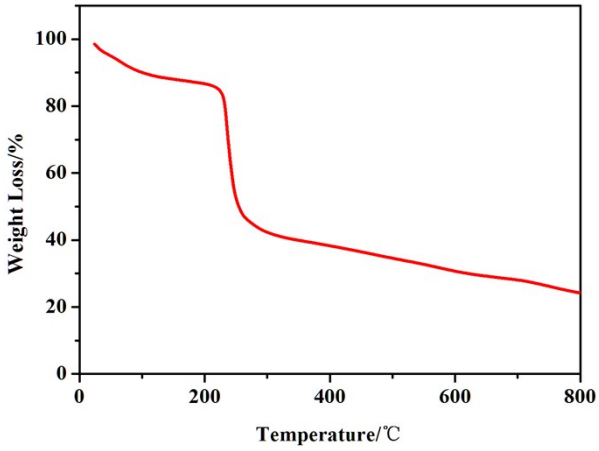

Figure S5. The TG curve of complex **3**.

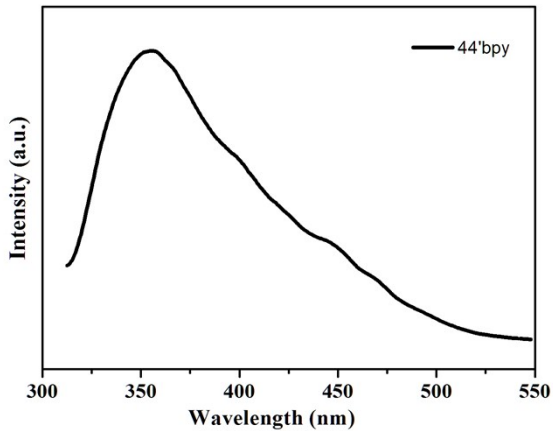

Figure S6. Solid-state fluorescent emissions for 4'4-bpy at room temperature.

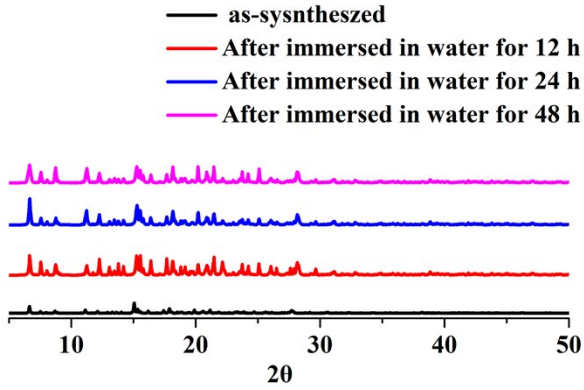

Figure S7. PXRD patterns of **3** after immersed in water solution for various conditions.

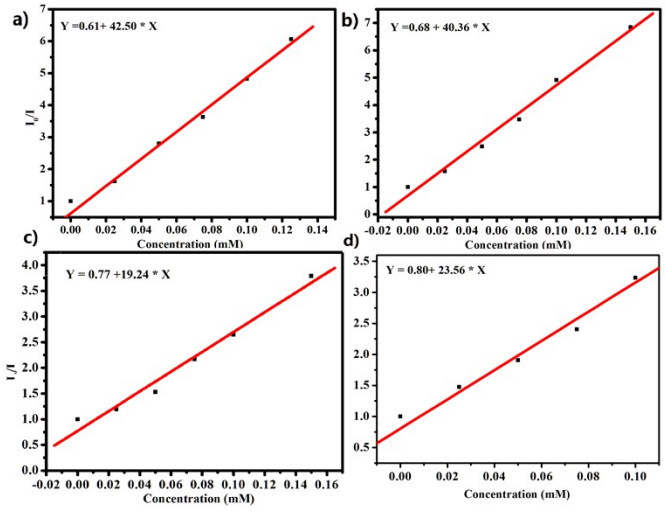

Figure S8. The K_{SV} plot for the fluorescence quenching of NT (a), NB (b), NP (c), NA (d) to aqueous@**3** suspensions at low concentration.

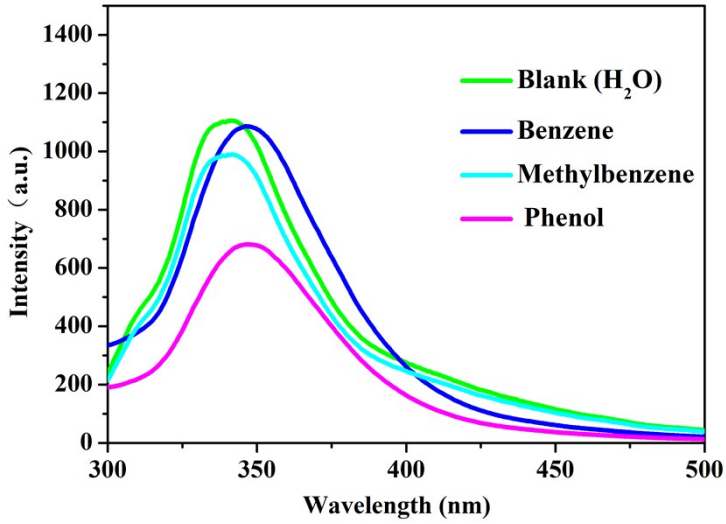

Figure S9. The photoluminesecence intensity of **3** dissolved in the aqueous with the addition of various aromatic hydrocarbon compounds.

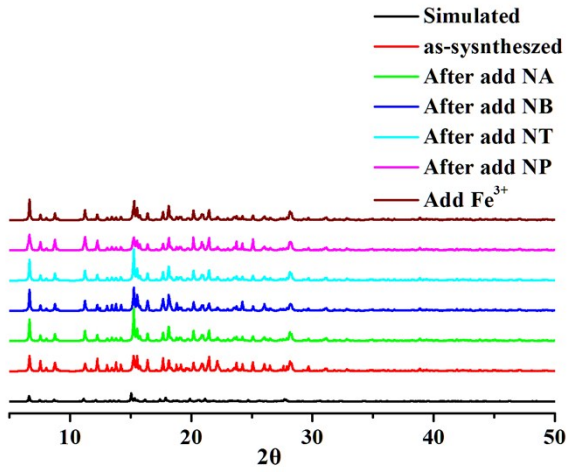

Figure S10. The PXRD patterns of **3** for the simulated, as-synthesized and after immerging in nitroaromatics and Fe^{3+} cations under water solutions.

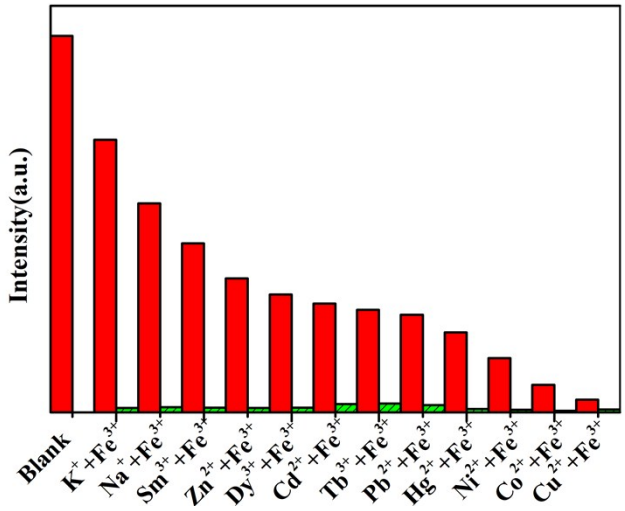

Figure S11. Comparison of the luminescence intensity of **3** in H_2O suspension with the introduction of other metal ions

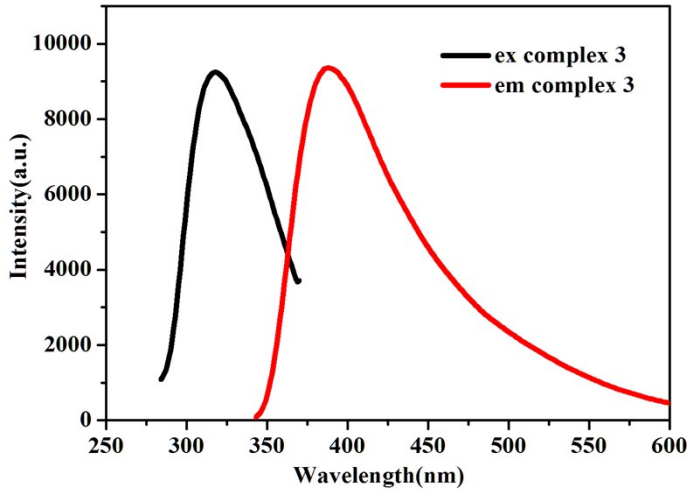

Figure S12. The exaction and emission of solid-state photoluminescence spectra of **3**.

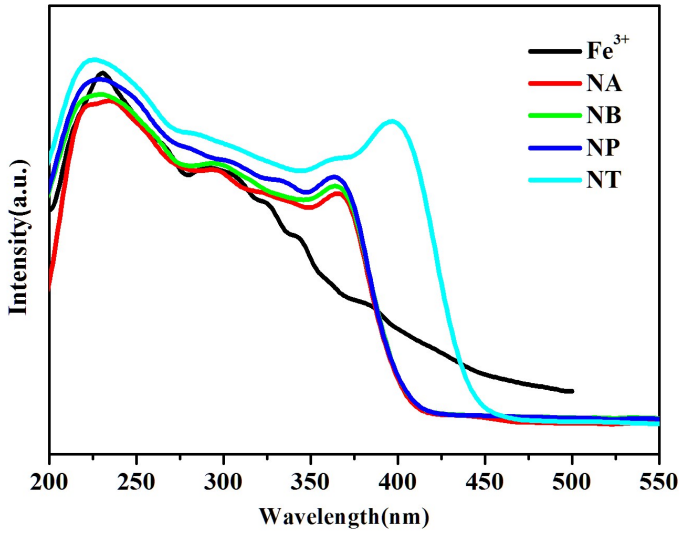

Figure S13. Spectral overlap between the normalized emission spectrum of **3** and normalized absorption spectra of the nitroaromatics and Fe^{3+} cations.